Second-Shell Hydrogen Bond Impacts Transition-State Structure in Bacillus subtilis Oxalate Decarboxylase

Wen Zhu,[†,§] Laurie A. Reinhardt,[‡,∥] and Nigel G. J. Richards*[,†]

[†]School of Chemistry, Cardiff University, Park Place, Cardiff CF10 3AT, United Kingdom

[‡]Institute for Enzyme Research and Department of Biochemistry, University of Wisconsin, Madison, Wisconsin 53726, United States

ABSTRACT: There is considerable interest in how "second-shell" interactions between protein side chains and metal ligands might modulate Mn(II) ion redox properties and reactivity in metalloenzymes. One such Mn-dependent enzyme is oxalate decarboxylase (OxDC), which catalyzes the disproportionation of oxalate monoanion into formate and CO_2. Electron paramagnetic resonance (EPR) studies have shown that a mononuclear Mn(III) ion is formed in OxDC during catalytic turnover and that the removal of a hydrogen bond between one of the metal ligands (Glu101) and a conserved, second-shell tryptophan residue (Trp132) gives rise to altered zero-field splitting parameters for the catalytically important Mn(II) ion. We now report heavy-atom kinetic isotope effect measurements on the W132F OxDC variant, which test the hypothesis that the Glu101/Trp132 hydrogen bond modulates the stability of the Mn(III) ion during catalytic turnover. Our results suggest that removing the Glu101/Trp132 hydrogen bond increases the energy of the oxalate radical intermediate from which decarboxylation takes place. This finding is consistent with a model in which the Glu101/Trp132 hydrogen bond in WT OxDC modulates the redox properties of the Mn(II) ion.

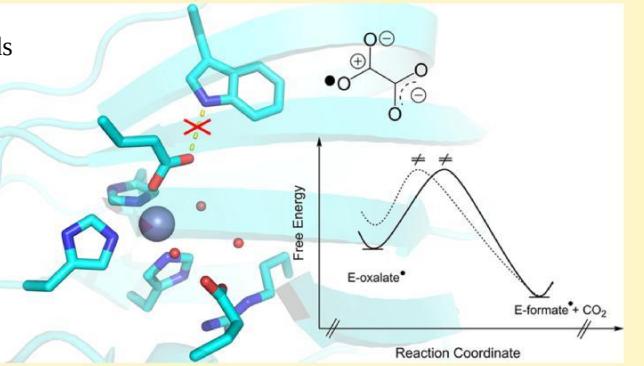

Oxalate decarboxylase (OxDC),[1] which catalyzes the disproportionation of oxalate monoanion into formate and CO_2 (Scheme 1), is one of only five enzymes that take advantage of redox changes in a mononuclear manganese center to mediate catalysis.[3]

Scheme 1. Reaction Catalyzed by Oxalate Decarboxylase (OxDC)[a]

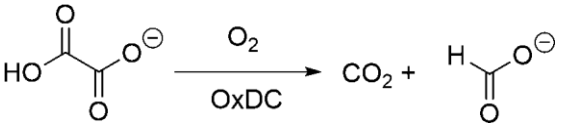

[a]Although the overall transformation is a disproportionation, catalytic activity requires dioxygen.

OxDC activity is solely Mn-dependent,[4,5] and recent electron paramagnetic resonance (EPR) studies have demonstrated the existence of enzyme-bound Mn(III) during catalytic turnover.[6,7] Current mechanistic models therefore assume that Mn(III) oxidizes oxalate to form a radical anion intermediate in which the barrier to decarboxylation is significantly lowered (Scheme 2).[8] The resulting Mn-bound radical anion intermediate then acquires an electron and a proton to regenerate Mn(III) and produce formate.

Although OxDC possesses two manganese-binding sites located in two cupin domains (Figure 1), substantial evidence exists to support the hypothesis that catalysis takes place only at the metal center located in the N-terminal domain of the enzyme.[9,10] In addition, the X-ray crystal structure of an Co(II)-substituted OxDC loop variant shows that oxalate coordinates the catalytically important manganese center in a monodentate fashion.[11] Maximal enzyme activity, however, also requires the presence of Mn(II) in the metal-binding site of the C-terminal cupin domain.[4] The apparent differential activity of the two Mn(II) centers in the enzyme is not understood.[12] It is possible, however, that "second-shell" interactions between protein side chains and metal ligands might modulate Mn(II) ion reactivity (Figure 1).[13] For example, the putative hydrogen bond between the Trp132 side chain and Glu101, which coordinates the metal ion, in the N-terminal Mn-binding site is replaced by an alternate hydrogen bond between the side chains of Gln232 and Glu280 in the C-terminal site (Bacillus subtilis numbering).

Removing the Glu101/Trp132 hydrogen bond by site-specific replacement of Trp132 by a phenylalanine residue leads to altered zero-field splitting parameters for the N-terminal Mn(II) ion as a result of altered charge density on the Glu101 carboxylate.[15] This observation has led to the proposal

Scheme 2. Current Model for the Catalytic Mechanism Used by OxDC[a]

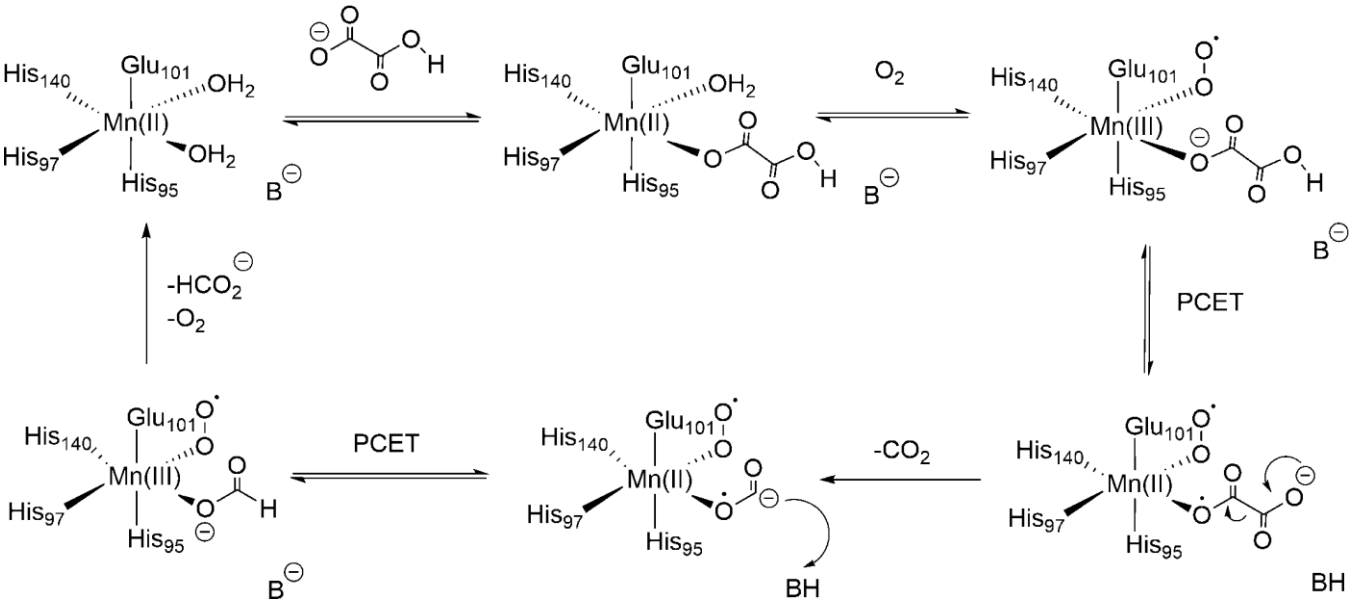

[a]Although dioxygen is assumed to be the reagent that oxidizes Mn(II) after substrate binding, the exact nature of the oxidizing agent remains to be determined. In addition, the proton-coupled electron transfers (PCETs) may proceed via independent electron-transfer and protonation steps. We assume that decarboxylation is irreversible. The identity of the general base (B) that removes the proton from the substrate monoanion is not yet determined.

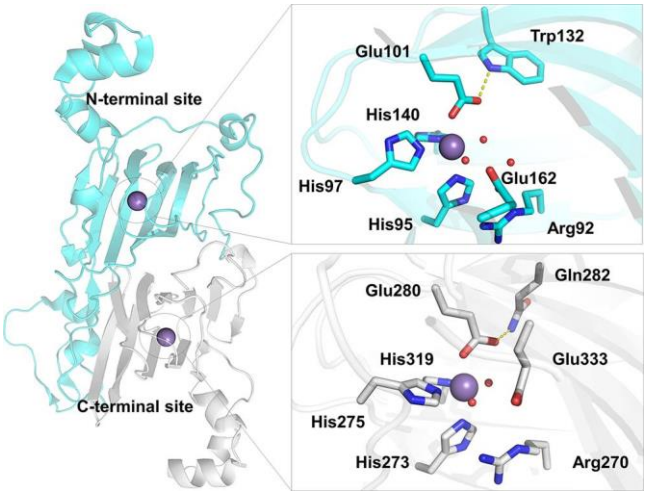

Figure 1. Mn(II)-binding sites present in the monomer of WT OxDC (PDB 1UW8). The enzyme is composed of two cupin domains, which are rendered in cyan (N-terminal) and gray (C-terminal). Active-site residue numbers are those for the OxDC present in Bacillus subtilis. Metal ions and water molecules are rendered as purple and red spheres, respectively, and the yellow dashed lines show second-shell hydrogen-bonding interactions.

that Mn(III) should be more stable in the W132F OxDC variant that in the WT enzyme. We now report heavy-atom kinetic isotope effect measurements that seek to test this idea. Our experimental measurements are consistent with a model in which removing the Glu101/Trp132 hydrogen bond results in altered bond polarization in the oxalate radical intermediate. This finding, in turn, suggests that the oxalate radical intermediate in the W132F OxDC variant is higher in energy than the cognate species formed in WT OxDC during turnover, consistent with the hypothesis that the Glu101/Trp132 hydrogen bond modulates the redox properties of the Mn(II) ion.

EXPERIMENTAL PROCEDURES

Materials. All chemicals and reagents were all purchased from Fisher Scientific (Pittsburgh, PA) or Sigma-Aldrich (St. Louis, MO), unless otherwise stated. Nickel-nitrilotriacetic acid agarose (Ni-NTA) was supplied by Qiagen (Germantown, MD), and BT Chelex 100 resin was purchased from Bio-Rad (Hercules, CA). Protein concentrations were determined using the CoomassiePlus Protein Assay reagent from ThermoFisher Scientific (Waltham, MA), and ICP-MS measurements were carried out at the Center for Applied Isotope Studies at the University of Georgia (Athens, GA).

Expression and Purification of the C-Terminally Tagged W132F OxDC Variant. A plasmid containing the gene encoding the C-terminally His_6-tagged W132F OxDC variant was generously provided by Dr. Whitney Kellett (Indiana University, Purdue University, Indianapolis, USA). After transformation in BL21 (DE3) Escherichia coli, the cells were grown at 37 °C until the OD_{600} reached 0.5. At this time, the cells were subjected to heat shock with continuous shaking at 42 °C for 15 min, and $MnCl_2$ (4 mM final concentration) was immediately supplied to the culture.[15] After induction with 0.8 mM IPTG, the C-terminally His_6-tagged W132F OxDC variant was purified by metal-affinity chromatography on a Ni-NTA column. Following elution with 250 mM imidazole and 500 mM NaCl in 50 mM phosphate buffer, pH 8.5, fractions of the desired protein (44 kDa on SDS-PAGE) were pooled and dialyzed against 50 mM Tris-Cl, pH 8.5, containing 500 mM NaCl. The protein solution was then shaken with 5% (w/v) BT Chelex 100-X resin for 2 h at 4 °C and concentrated (Amicon Ultra 30K, Millipore) to 5 mg/mL. The enzyme concentration was determined by Bradford assay using bovine serum albumin as the standard.[16]

Steady-State Enzyme Assays. OxDC activity was measured using a standard end-point, coupled assay with formate dehydrogenase (FDH) in which NADH production was monitored at 340 nm.[17] Thus OxDC (5.5 μM) was incubated for 1 min with varying amounts of potassium oxalate (0−200 mM, pH 4.2) in 50 mM acetate buffer, pH 4.2, containing 0.5 mM o-phenylenediamine and 0.2% TritonX. After quenching the reaction by the addition of 0.1 M NaOH, the resulting solution was incubated overnight at 37 °C in the presence of FDH and NAD^+ (1.5 mM final concentration). The absorbance at 340 nm was then converted to NADH concentration using a standard curve. Measurements were made at specific substrate and enzyme concentrations in triplicate. All data were processed using GraphPad Prism and analyzed by standard methods to obtain the values of V and V/K.[18]

Kinetic Isotope Effect Nomenclature. In this paper, $^{13}(V/K)$ represents the ratio of V/K for the ^{12}C-containing substrate relative to the ^{13}C-containing substrate.[19] In a similar manner, $^{18}(V/K)$ represents the ratio of V/K for the ^{16}O-containing substrate relative to the ^{18}O-containing substrate.

^{13}C and ^{18}O Kinetic Isotope Effect Measurements. As described in detail elsewhere,[17] the internal competition method[20] was used to determine the primary ^{13}C and secondary ^{18}O isotope effects on the decarboxylation reaction catalyzed by the W132F OxDC variant. All experiments employed oxalate in which the heavy-atom isotopes were at natural abundance. Partial and total conversion reactions at 22 °C were performed at either pH 4.2 or pH 5.7 using 100 mM 1,4-bis(2-hydroxyethyl)-piperazine (BHEP) or 100 mM piperazine, respectively. All buffer solutions contained 0.5 mM o-phenylenediamine and were sparged with N_2(g) for 1 h before use to remove adventitious CO_2 in solution. Similarly, all gases were passed over Ascarite to remove CO_2(g) prior to use. Solutions of 40 mM potassium oxalate dissolved in the appropriate buffer, which had been sparged with O_2(g) for 1 h prior to use, were placed in a sealed flask. Reactions were initiated by the addition of enzyme in N_2-saturated buffer and subsequently quenched by the addition of 500 mM Tris-Cl, pH 7.5. Incubation times were varied from 37 min to 3 h so as to obtain mixtures in which a different fraction of reaction had taken place. Complete oxalate consumption required incubation with the W132F OxDC variant at 22 °C for 14 h in either of the two buffers. CO_2 produced during the reaction was collected and purified through a vacuum line, and the isotopic composition was determined using an isotope ratio mass spectrometer (IRMS). After quenching, the solution was passed through an Amicon ultrafiltration system to remove enzyme, and an aliquot (50 μL) was taken to determine the fraction of conversion, f, using an oxalate assay kit (Trinity Biotech, NY). In addition, formate produced in the reaction was measured using the standard FDH-based assay outlined above.

The isotopic composition of residual oxalate and formate produced in the reaction was also determined in these studies. Thus formate and oxalate were separated by anion-exchange chromatography (Bio-Rad AG-1 resin) using dilute H_2SO_4, pH 2.7, as eluent. Fractions that contained either oxalate or formate were pooled, and the pH of these solutions was adjusted to neutral pH using 0.1 N NaOH before the volume was reduced. After sparging with N_2(g) for 30 min, water was removed completely from the resulting solutions by heating overnight at 70 °C under high vacuum. DMSO (2 mL) containing I_2 (250−400 mg) was then used to oxidize the dried samples of oxalate or formate (45 min) with the isotopic composition of the CO_2 produced in the reaction being measured by IRMS. Control experiments were performed at pH 4.2 using 2% $H_2{}^{18}O$ to examine whether $^{18}O/^{16}O$ exchange took place between solvent water and either the substrate or products under the reaction conditions. The observed isotope effects were analyzed using procedures that our group has detailed elsewhere.[17,21]

RESULTS AND DISCUSSION

Standard measurements of formate production at pH 4.2 gave steady-state kinetic parameters for the W132F OxDC variant and indicated that the removal of the Glu101/Trp132 hydrogen bond had little impact on the turnover number of the enzyme (Table 1). On the contrary, the oxalate K_M was increased approximately seven-fold, leading to a decrease in k_{cat}/K_M/Mn. To obtain more detail about the effects of this mutation on catalysis, we determined the primary ^{13}C and secondary ^{18}O isotope effects (IEs) for the W132F-catalyzed decarboxylation by internal competition using oxalate in which the heavy-atom isotopomers were at natural abundance (Table 2). As discussed elsewhere,[20] these measurements report on isotopically sensitive steps in the catalytic mechanism up to, and including, the first irreversible step, which we assume to be CO_2 formation. Given that CO_2 hydration and isotope exchange might have impacted the ^{18}O IEs at pH 5.7 differently from those at pH 4.2, control experiments using 2% $H_2{}^{18}O$ in the solvent were performed. These studies showed that our results were not severely affected by $^{18}O/^{16}O$ isotope exchange between substrate and water, especially when the reaction was carried at pH 4.2. On the contrary, in analyzing the observed isotope effects, the ^{13}C IEs are viewed as providing more reliable and accurate values. $^{13}(V/K)$ on CO_2 is 1.3% at pH 5.7 in the W132F-catalyzed decarboxylation, which is substantially larger than that observed for WT OxDC (0.8%), and $^{13}(V/K)$ on formate is 3.6% as compared with 1.9% measured for WT OxDC. Given that $^{13}(V/K)$ is 3−5% for decarboxylases in which the loss of CO_2 is rate-limiting,[22] our values indicate that the observed IEs arise from two (or more) steps that are sensitive to isotopic substitution. As in previous work from our laboratory,[17,21] we interpreted the observed IEs using a minimal kinetic model (Scheme 3) in which an initial proton-coupled electron transfer (PCET) takes place after oxalate binding to give an intermediate that then undergoes irreversible decarboxylation. The discrepancy in the two $^{13}(V/K)$ values is therefore associated with different sensitivities to isotopic substitution of the two carbon atoms in the step(s) preceding C−C bond cleavage.[17]

Table 1. Steady-State Kinetic Parameters for the Decarboxylation Reaction Catalyzed by Recombinant, WT OxDC, and the C-Terminally His_6-Tagged W132F OxDC Variant at pH 4.2 and 25 °C

enzyme	K_M (mM)	k_{cat} (s^{-1})	k_{cat}/K_M/Mn (M^{-1} s^{-1})	Mn content
WT OxDC	4.0 ± 0.5	60 ± 2	10 000 ± 1000	1.6
W132F OxDC	27 ± 5	60 ± 4	1300 ± 300	1.8

Analysis of the Observed $^{13}(V/K)$ and $^{18}(V/K)$ Isotope Effects. To understand how the commitments to catalysis might have been altered by the removal of the Glu101/Trp132 hydrogen bond, we undertook a quantitative analysis of the

Table 2. ^{13}C and ^{18}O Isotope Effects on the Reactions Catalyzed by Recombinant, C-Terminally His$_6$-Tagged WT OxDC, and the W132F and T165V OxDC Variants at 22 °C[a]

		^{13}(V/K)		^{18}(V/K)		
OxDC variant	pH	CO_2	HCO_2^-	CO_2	HCO_2^-	citation
WT	4.2	1.005 ± 0.001	1.015 ± 0.001	0.998 ± 0.002	1.011 ± 0.002	17
W132F	4.2	1.010 ± 0.001	1.024 ± 0.001	0.993 ± 0.001	1.009 ± 0.001	
T165V	4.2	0.998 ± 0.001	1.008 ± 0.001	0.991 ± 0.001	1.004 ± 0.001	15
WT	5.7	1.008 ± 0.001	1.019 ± 0.001	0.993 ± 0.002	1.010 ± 0.001	17
W132F	5.7	1.013 ± 0.001	1.036 ± 0.001	0.989 ± 0.002	1.014 ± 0.002	
T165V	5.7	0.997 ± 0.001	1.009 ± 0.001	0.984 ± 0.001	1.006 ± 0.001	15

[a]Data for WT OxDC and the T165V OxDC variant have been previously published[15,17] and are included here for ease of comparison.

Scheme 3. Minimal Kinetic Model for the OxDC-Catalyzed Reaction Used in the Quantitative Interpretation of the ^{13}C and ^{18}O Isotope Effects[15,17,21]

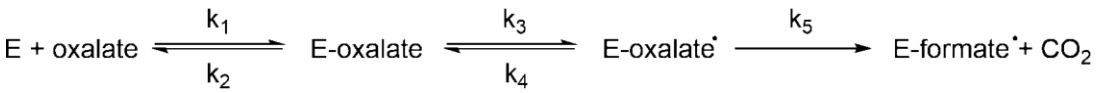

data using our minimal kinetic model and the following equation

$$ {}^{x}(V/K) = \frac{{}^{x}K_{eq3}\,{}^{x}k_5\,k_3 + \left(\frac{k_5}{k_4}\right) + \frac{k_3k_5}{k_2k_4}}{1 + \left(\frac{k_5}{k_4}\right)\left(1 + \frac{k_3}{k_2}\right)} \quad (1) $$

where ^{x}(V/K) is the ratio of V/K for the lighter isotopomer in the enzyme-catalyzed reaction relative to that for the heavy isotopomer (x = 13 or 18). k_3, k_4, and k_5 are rate constants in the minimal model that are assumed to be sensitive to isotopic substitution, and $^{x}k_3$ and $^{x}k_5$ are the isotope effects on the formation of oxalate radical anion and decarboxylation, respectively. Finally, $^{13}K_{eq3}$ and $^{18}K_{eq3}$ are ^{13}C and ^{18}O equilibrium isotope effects (EIEs) on the putative oxalate radical anion intermediate. The derivation of this equation and a full discussion of many of the assumptions used below in analyzing the IE data for the reaction catalyzed by the W132F OxDC variant have been discussed elsewhere.[17] For example, we assume that oxalate monoanion remains the substrate when the Glu101/Trp132 hydrogen bond is absent in the active site and that the catalytic mechanism is unaffected by the introduction of a phenylalanine residue. As a result, and in a similar manner to WT OxDC, the initial rate of the T132F-catalyzed reaction is slower at pH 5.7 because of the increased concentration of the oxalate dianion in solution.[17]

CO_2-Based Analysis. As discussed in detail elsewhere,[17] in analyzing the ^{13}(V/K) IE value on CO_2 at pH 5.7, we assume that k_3/k_2 can be ignored, that $^{13}k_5$ on CO_2 during decarboxylation is 1.04 (which is an average value for this reaction[17,22]), and that $^{13}K_{eq3}$ and $^{13}k_3$ are both unity; that is, proton removal from the carboxylic acid is assumed to proceed with a negligible ^{13}C isotope effect.[23] We therefore obtain the following expression

$$ {}^{13}(V/K) = \frac{1.04 + \left(\frac{k_5}{k_4}\right)}{1 + \left(\frac{k_5}{k_4}\right)} = 1.013 \quad (2) $$

Solving this equation yields a value of $k_5/k_4 = 2.08$ (Table 3), which differs from the value of $k_5/k_4 = 4.00$ determined for WT OxDC under the same conditions. The reduction in the commitment factor for the W132F OxDC variant is associated with an increase in the k_4 rate constant because, for reasons that are discussed below, the magnitude of k_5 is increased compared with the cognate rate constants in the reaction catalyzed by WT OxDC (Table 3).

Table 3. Commitment Factors and C−O Bond Orders (See Text) in the Decarboxylation Transition States for the Reactions Catalyzed by WT OxDC and the W132F and T165V OxDC Variants[a]

enzyme	k_3/k_2	k_5/k_4	$^{13}K_{eq3}$	$^{18}k_3$	C−O bond order	citation
WT OxDC	0.75	4.00	1.021	1.016	1.15	17
W132F OxDC	0.44	2.08	1.039	1.012	0.97	
T165V OxDC	3.29	12.33	1.013	1.004	1.26	15

[a]Data for WT OxDC and the T165V OxDC variant have been previously published and are included here for ease of comparison.

Given that the carboxylic acid at the end of the substrate that becomes CO_2 is protonated in our mechanistic model, the ^{18}(V/K) value on CO_2 at pH 5.7 must be multiplied by 0.98.[17] In addition, $^{18}K_{eq3}$ is assigned a value of 1.02 as a result of proton removal in the step(s), leading to the formation of the oxalate radical anion.[17] These assumptions then yield the following equation

$$ {}^{18}(V/K) = \frac{0.98[(1.02)(0.9835) + {}^{18}k_3(2.077)]}{1 + 2.077} = 0.989 \quad (3) $$

making the additional assumptions that (i) k_3/k_2 is small enough to ignore at pH 5.7 and (ii) the IE on decarboxylation is midway between an estimated $^{18}K_{eq5}$ (0.967) and unity.[17] As a result, we obtain a value of 1.0121 for $^{18}k_3$, which is a reasonable value for the deprotonation step, albeit smaller than the value of 1.0159 computed for WT OxDC at pH 5.7 (Table 3).

Formate-Based Analysis. In the case of ^{13}(V/K) on formate at 5.7, we can write the following equation

$$ {}^{13}(V/K) = \frac{(1.03)\,{}^{13}K_{eq3} + (2.08)\frac{{}^{13}K_{eq3} + 1}{2}}{1 + 2.08} = 1.036 \quad (4) $$

where we again ignore k_3/k_2 and assume that (i) k_5/k_4 has a value of 2.08 as derived in the CO_2 analysis (see above), (ii)

$^{13}k_3$ lies midway between $^{13}K_{eq3}$ and unity,[17] and (iii) $^{13}k_5$ for decarboxylation is 1.03. The latter value reflects the fact that the change in bond order at this carbon is less than that at the carbon, which becomes CO_2. Solving the resulting equation gives a value of 1.039 for $^{13}K_{eq3}$ and a C−O bond order in the transition state of 0.88 based on calculations of the dependence of fractionation factor upon C−O bond order that we have previously reported.[17] Of course, it is possible that assumption (ii), which was used in our original study on WT OxDC to simplify data analysis,[17] may be incorrect for the reaction catalyzed by the W132F OxDC variant. We therefore examined the effect of setting $^{13}k_3$ to $^{13}K_{eq3}$ in our analysis. Setting $^{13}k_3$ to $^{13}K_{eq3}$ and solving gives $^{13}K_{eq3} = 1.026$ and a corresponding C−O bond order of 1.09, which is still smaller than the bond order computed for WT OxDC (1.16).[17] Moreover, because we have shown the chemical bonding in oxalate and the oxalate radical anion to differ on the basis of high-level ab initio calculations,[8] and due to the fact that a larger IE is observed for the W132F OxDC variant, $^{13}k_3$ is unlikely to be unity. Thus our conclusions are unaffected, and, for the sake of comparison, we compare the IE data for WT OxDC and the W132F OxDC variant using an identical set of assumptions.

An alternate estimate of the C−O bond order could be obtained by determining the value of $^{18}K_{eq3}$ using the following equation

$$^{18}(V/K) = \frac{(1.003)^{18}K_{eq3} + (2.08)^{\frac{^{18}K_{eq3}+1}{2}}}{1 + 2.08} = 1.014 \quad (5)$$

where we assume that (i) $^{18}k_3$ lies midway between $^{18}K_{eq3}$ and unity, (ii) $^{18}k_5 = 1.003$ due to the bond angle change in the formate radical intermediate,[17] and (iii) k_3/k_2 is small enough to be ignored. Solving this equation gives a value of 1.02 for $^{18}K_{eq3}$, which corresponds to a C−O bond order of 1.054. Taking the average of the estimates obtained from the $^{13}K_{eq3}$ and $^{18}K_{eq3}$ values then yields an estimate of 0.97 for the C−O bond order, considerably smaller than 1.15 estimated for the transition state in the reaction catalyzed by WT OxDC (Table 3). We therefore conclude that the oxalate radical anion in the W132F-catalyzed reaction can be represented solely by resonance form I (see below) in which a full positive charge is located on the carbon that is finally converted into formate.

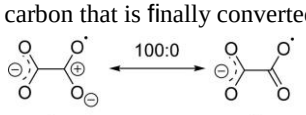

I II

The C−O bonds in this Mn-bound carboxylate are therefore considerably more polarized than the cognate bonds in the radical anion intermediate formed during the reaction catalyzed by WT OxDC (1.15).[17] As a result, the carbon atom is more electron-deficient, which will promote C−C bond cleavage and hence increase the magnitude of the k_5 rate constant. Thus the increase in k_4 must be greater to give a lower k_5/k_4 ratio in the W132F-catalyzed transformation; therefore, we propose that the removal of the Glu101/Trp132 hydrogen bond raises the energy of the putative oxalate-based radical intermediate (Scheme 2).

At pH 4.2, the smaller observed values of the heavy atom IEs suggest that k_3/k_2 is no longer negligible. We therefore repeated our calculations to obtain an estimate of this commitment factor. For the end of the substrate that becomes CO_2, substitution of the observed $^{13}(V/K)$ value at pH 4.2 gives the following expression

$$^{13}(V/K) = \frac{(1.04) + (2.077)\left(1 + \frac{k_3}{k_2}\right)}{1 + (2.077)\left(1 + \frac{k_3}{k_2}\right)} = 1.01 \quad (6)$$

where $^{13}k_5$ on CO_2 for the decarboxylation step is assumed to be 1.04, (ii) k_5/k_4 has the same value as at pH 5.7, and (iii) $^{13}K_{eq3}$ and $^{13}k_3$ are both unity.[17] Solving this equation gives $k_3/k_2 = 0.44$, which is smaller than that observed for WT OxDC (0.75) (Table 3). Given that K_M is larger for the W132F OxDC variant, an increase in the k_2 value might be expected, although the k_3 rate constant may also be smaller given that the oxalate-based radical intermediate has a higher energy (see above).

With estimates for $^{13}k_3$, k_3/k_2, k_5/k_4, and $^{13}K_{eq3}$ in hand, we calculated the value of $^{13}(V/K)$ on formate at pH 4.2 to evaluate the validity of using our minimal kinetic model to interpret the observed IEs. Substitution of the $^{13}k_3$, k_3/k_2, k_5/k_4, and $^{13}K_{eq3}$ values into the master equation gave an estimate of 1.027 for $^{13}(V/K)$, which is in good agreement with that observed experimentally (1.026) (Table 2) and confirms that the catalytic mechanism is unchanged by the removal of the Glu101/Trp132 hydrogen bond.

Second-Shell Interactions in OxDC and Their Impact on the Energy of the Oxalate Radical Anion Intermediate and the Barrier to Decarboxylation. The role of noncovalent interactions between residue side chains in the local protein environment and the ligands that coordinate metal ions is of considerable general interest, especially for the development of transition-metal complexes with novel catalytic activities. In the case of OxDC, questions remain about how Mn(III) is generated during turnover and how its intrinsic activity as an oxidizing agent is controlled by the metal ligands or oxalate binding. Given that Trp132 (Bacillus subtilis numbering) is conserved in all known oxalate decarboxylases and forms a hydrogen bond with the metal ligand Glu101, we speculated that removing this interaction would impact the energy difference between Mn(III)-bound oxalate and the Mn(II)-bound oxalate radical anion intermediate. Importantly, the X-ray crystal structure of the Co-substituted W132F OxDC variant (PDB: 4MET) shows that removing the Glu101/Trp132 hydrogen bond has no impact on the overall fold of the enzyme, and the aromatic rings of Phe132 and Trp132 are positioned identically in the N-terminal Mn(II)-binding site (Figure 2).

On the contrary, there is a slight alteration in the position of the Glu-162 side chain and a rotation of the imidazole ring in the metal ligand His-97. This modification of metal coordination is likely associated with substituting Co(II) for Mn(II),[14] however, and so we assume that the geometry of the Mn/ligand interactions is unchanged by the removal of the Glu-101/Trp-132 hydrogen bond. We also note that removing the Glu101/Trp132 hydrogen bond perturbs the number and locations of active-site water molecules in the W132F OxDC variant compared with WT OxDC (Figure 2). Thus the Mn-bound water oxygens in the W132F variant occupy equivalent positions to the oxygen atoms of oxalate and Mn-bound water seen in the X-ray crystal structure of an OxDC variant in which Glu162 is deleted (PDB 5HI0).[11]

Despite these small alterations in active-site geometry, however, the absence of the second-shell Glu101/Trp132 hydrogen bond does impact the partition ratios k_5/k_4 and k_3/k_2 relative to those determined for WT OxDC (Table 3). Our working hypothesis is that removing the hydrogen bond

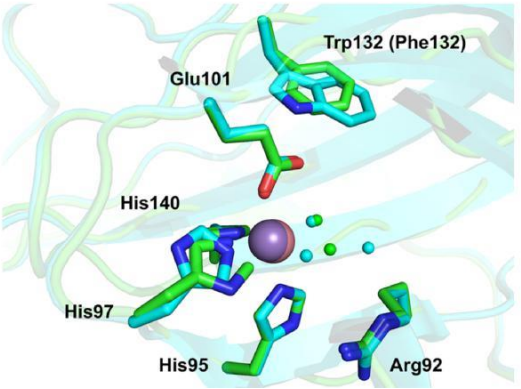

Figure 2. Superimposition of the X-ray crystal structures of WT OxDC (PDB 1UW8) and the Co-substituted W132F OxDC variant (PDB 4MET).The ring "flip" seen for His97 in the W132F OxDC variant likely results from metal replacement, as discussed elsewhere.[11,14] Carbon atoms in WT OxDC and the W132F OxDC variant are rendered in cyan and green, respectively. Metal ions are shown as purple (WT OxDC) and salmon (W132F) spheres, and active-site waters are rendered as cyan (WT OxDC) and green (W132F) spheres.

increases the charge density on the Glu101 side chain with a concomitant change in the metal midpoint potential so that Mn(III) is more stable in the W132F OxDC variant compared with the WT enzyme. As a result, we would expect that the rate constant, k_3, for the formation of the oxalate-based radical to be decreased and the energy of the Mn(II)/oxalate radical intermediate to be increased, thereby increasing the rate of reversion (k_4) back to the Michaelis complex and Mn(III). The higher energy of the Mn-bound oxalate-based radical intermediate in the W132F OxDC variant is also consistent with the larger magnitude of the decarboxylation rate constant k_5 in that decarboxylation proceeds through an "earlier" transition state in which the C−O bonds at the carbon proximal to the metal are more polarized (Figure 3). We note that the oxalate radical anion intermediate formed in the reaction catalyzed by WT OxDC can be considered as a 70:30 mixture of the resonance structures I and II (see above),[17] and heavy-atom IE measurements on the reaction catalyzed by the R92K OxDC variant support the view that decarboxylation is slower when resonance structure II makes a larger contribution to the transition-state structure; that is, there is less C−O bond polarization.[21]

These findings for the W132F OxDC variant contrast with those that we have reported for the T165V OxDC variant in which the Arg92/Thr165 hydrogen bond is removed by site specific substitution of Thr165 by a valine residue (Figure 4).[15] Thus both partition ratios k_5/k_4 and k_3/k_2 are decreased in this variant relative to those determined for WT OxDC (Table 3), suggesting that the oxalate-based radical intermediate becomes more stable (Figure 5). As a result, the removal of Arg92/Thr165 hydrogen bond results in decarboxylation proceeding via a "later" transition state, as evidenced by the increased bond order (1.26) and lower polarization of the C−O bonds at the carbon proximal to the metal in the T165V OxDC variant.[15]

CONCLUSIONS

The functional roles of second-shell residues in metalloenzyme catalysis is receiving increased attention,[24,25] and may underlie the inability of simple Mn(II)-containing complexes to mediate cleavage of the C−C bond in oxalate.[26] Indeed, the heavy-atom isotope effect measurements reported herein clearly demonstrate the importance of individual hydrogen bonds in the OxDC active site for determining transition-state structure and the free energy of radical intermediates in the catalytic mechanism. In part, these effects may result from these small active-site changes in modulating the midpoint potential of Mn(II) in the N-terminal domain of OxDC, although further

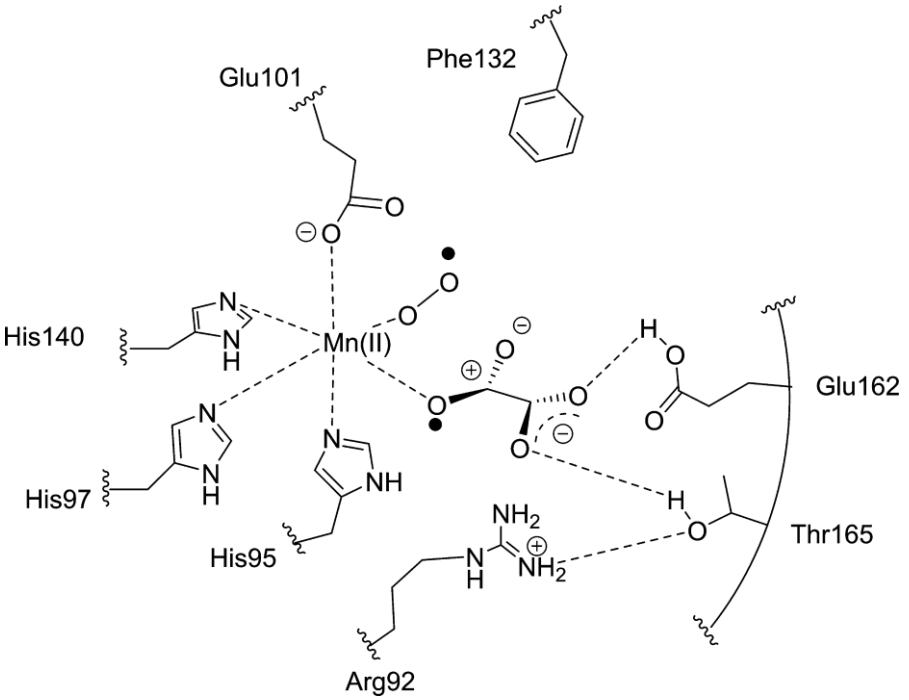

Figure 3. Model for the radical anion intermediate in the W132F OxDC variant..

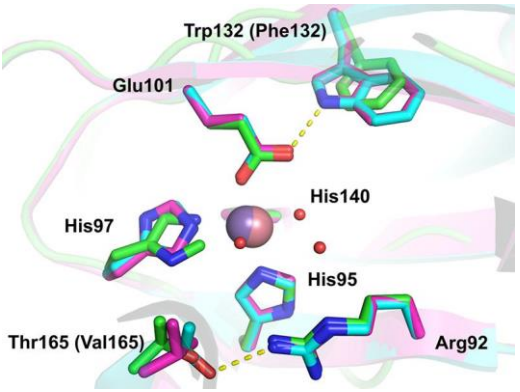

Figure 4. Superimposition of the X-ray crystal structures of WT OxDC (PDB 1UW8) and the T165V (PDB 3S0M) and co-substituted W132F OxDC (PDB 4MET) variants. Note that the removal of the Arg92/Thr165 or Glu101/Trp132 hydrogen bonds does not impact the positions of other active-site residues. Carbon atoms in WT OxDC are rendered in cyan. Carbon atoms in the T165V and the co-substituted W132F OxDC variants are rendered in magenta and green, respectively. Metal ions are shown as purple (WT OxDC and the T165V OxDC variant) and salmon (W132F) spheres, and the three active-site waters in WT OxDC are shown as red spheres.

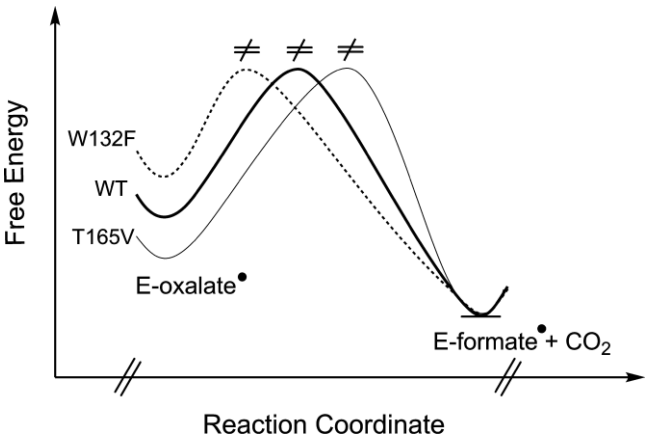

Figure 5. Qualitative representation of the decarboxylation free energy barriers in WT OxDC (thick line) and the W132F (dashed line) and T165V (thin line) OxDC variants.

studies will be needed to determine the validity of this hypothesis and the magnitude of such changes.

AUTHOR INFORMATION

Corresponding Author

*E-mail: RichardsN14@cardiff.ac.uk.

ORCID

Wen Zhu: 0000-0003-3190-0071

Laurie A. Reinhardt: 0000-0002-5488-0440

Nigel G. J. Richards: 0000-0002-0375-0881

Present Addresses

§ W.Z.: Department of Chemistry and California Institute for Quantitative Biosciences, 631 Stanley Hall, University of California, Berkeley, California 94720-3220, United States.

∥ L.A.Z.: U.S. Dairy Forage Research Center, 1925 Linden Drive West, Madison, Wisconsin 53706, United States.

Funding

This work was supported by NIH grant DK061666 (N.G.J.R.) and the School of Chemistry, Cardiff University.

Notes

The authors declare no competing financial interest.

ACKNOWLEDGMENTS

We thank Professor Judith P. Klinman for useful discussions about this work and Dr. Whitney Kellett for providing a construct for the expression of the W132F OxDC variant.

DEDICATION

This paper is dedicated to the memory of W. W. Cleland (1930−2013).

ABBREVIATIONS

OxDC, oxalate decarboxylase; MD, molecular dynamics; FDH, formate dehydrogenase; BHEP, 1,4-bis(2-hydroxyethyl)-piperazine; IRMS, isotope ratio mass spectrometer; IE, isotope effect.

REFERENCES

(1) Shimazono, H. (1955) Oxalic acid decarboxylase, a new enzyme from the mycelium of wood destroying fungi. J. Biochem. 42, 321−340.

(2) Svedruzic, D., Jonsson, S., Toyota, C. G., Reinhardt, L. A., Ricagno, S., Lindqvist, Y., and Richards, N. G. J. (2005) The enzymes of oxalate metabolism: unexpected structures and mechanisms,. Arch. Biochem. Biophys. 433, 176−192.

(3) Zhu, W., and Richards, N. G. J. (2017) Biological functions controlled by manganese redox changes. Essays Biochem. 61, 259−270.

(4) Moomaw, E. W., Angerhofer, A., Moussatche, P., Ozarowski, A., Garcia-Rubio, I., and Richards, N. G. J. (2009) Metal dependence of oxalate decarboxylase activity. Biochemistry 48, 6116−6125.

(5) Tanner, A., Bowater, L., Fairhurst, S. A., and Bornemann, S. (2001) Oxalate decarboxylase requires manganese and dioxygen for activity. J. Biol. Chem. 276, 43627−43634.

(6) Zhu, W., Wilcoxen, J., Britt, R. D., and Richards, N. G. J. (2016) Formation of hexacoordinate Mn(III) in Bacillus subtilis oxalate decarboxylase requires catalytic turnover. Biochemistry 55, 429−434.

(7) Twahir, U. T., Ozarowski, A., and Angerhofer, A. (2016) Redox cycling, pH dependence, and ligand effects of Mn(III) in oxalate decarboxylase from Bacillus subtilis. Biochemistry 55, 6505−6516.

(8) Molt, R. W., Jr., Lecher, A. M., Clark, T., Bartlett, R. J., and Richards, N. G. J. (2015) Facile C_{sp2}-C_{sp2} bond cleavage in oxalic acid-derived radicals. J. Am. Chem. Soc. 137, 3248−3252.

(9) Just, V. J., Burrell, M. R., Bowater, L., McRobbie, I., Stevenson, C. E., Lawson, D. M., and Bornemann, S. (2007) The identity of the active site of oxalate decarboxylase and the importance of the stability of active-site lid conformations,. Biochem. J. 407, 397−406.

(10) Just, V. J., Stevenson, C. E., Bowater, L., Tanner, A., Lawson, D. M., and Bornemann, S. (2004) A closed conformation of Bacillus subtilis oxalate decarboxylase OxDc provides evidence for the true identity of the active site,. J. Biol. Chem. 279, 19867−19874.

(11) Zhu, W., Easthon, L. M., Reinhardt, L. A., Tu, C.-K., Cohen, S. E., Silverman, D. N., Allen, K. N., and Richards, N. G. J. (2016) Substrate binding mode and molecular basis of a specificity switch in oxalate decarboxylase. Biochemistry 55, 2163−2173.

(12) Karmakar, T., Periyasamy, G., and Balasubramanian, S. (2013) CO_2 migration pathways in oxalate decarboxylase and clues about its active site. J. Phys. Chem. B 117, 12451−12460.

(13) Miller, A.-F. (2008) Redox tuning over almost 1 V in a structurally conserved active site: Lessons from Fe-containing superoxide dismutase. Acc. Chem. Res. 41, 501−510.

(14) Campomanes, P., Kellett, W. F., Easthon, L. M., Ozarowski, A., Allen, K. N., Angerhofer, A., Rothlisberger, U., and Richards, N. G. J. (2014) Assigning the EPR fine structure parameters of the Mn(II) centers in Bacillus subtilis oxalate decarboxylase by site-directed mutagenesis and DFT/MM calculations. J. Am. Chem. Soc. 136, 2313−2323.

(15) Saylor, B. T., Reinhardt, L. A., Lu, Z., Shukla, M. S., Nguyen, L., Cleland, W. W., Angerhofer, A., Allen, K. N., and Richards, N. G. J. (2012) A structural element that facilitates proton-coupled electron transfer in oxalate decarboxylase,. Biochemistry 51, 2911−2920.
(16) Bradford, M. M. (1976) A rapid and sensitive method for the quantitation of microgram quantities of protein utilizing the principle of protein-dye binding,. Anal. Biochem. 72, 248−254.
(17) Reinhardt, L. A., Svedruzic, D., Chang, C. H., Cleland, W. W., and Richards, N. G. J. (2003) Heavy atom isotope effects on the reaction catalyzed by the oxalate decarboxylase from Bacillus subtilis. J. Am. Chem. Soc. 125, 1244−1252.
(18) Cleland, W. W. (1979) Statistical analysis of enzyme kinetic data. Methods Enzymol. 63, 103−138.
(19) Northrop, D. B. (1977) Determining the Absolute Magnitude of Hydrogen Isotope Effects, in Isotope Effects on Enzyme-Catalyzed Reactions (Cleland, W. W., O'Leary, W. H., and Northrop, D. B., Eds.) pp 122−152, University Park Press, Baltimore, MD.
(20) Weiss, P. M. (1991) Heavy-Atom Isotope Effects Using the Isotope-Ratio Mass Spectrometer, in Enzyme Mechanism from Isotope Effects (Cook, P. F., Ed.) pp 292−311, CRC Press, Boca Raton, FL.
(21) Svedruzic, D., Liu, Y., Reinhardt, L. A., Wroclawska, E., Cleland, W. W., and Richards, N. G. J. (2007) Investigating the roles of putative active site residues in the oxalate decarboxylase from Bacillus subtilis, Arch. Arch. Biochem. Biophys. 464, 36−47.
(22) O'Leary, M. H. (1980) Determination of heavy atom isotope effects on enzyme-catalyzed reactions. Methods Enzymol. 64, 83−104.
(23) Bayles, J. W., Bron, J., and Paul, S. O. (1976) Secondary carbon-13 isotope effect on the ionization of benzoic acid. J. Chem. Soc., Faraday Trans. 1 72, 1546−1552.
(24) Genna, V., Colombo, M., De Vivo, M., and Marcia, M. (2018) Second-shell basic residues expand the two-metal-ion architecture of DNA and RNA processing enzymes. Structure 26, 40−50.
(25) Vogt, L., Vinyard, D. J., Khan, S., and Brudvig, G. W. (2015) Oxygen-evolving complex of photosystem II: an analysis of second-shell residues and hydrogen-bonding networks. Curr. Opin. Chem. Biol. 25, 152−158.
(26) Scarpellini, M., Gatjens, J., Martin, O. J., Kampf, J. W., Sherman, S. E., and Pecoraro, V. L. (2008) Modeling the resting state of oxalate oxidase and oxalate decarboxylase enzymes. Inorg. Chem. 47, 3584−3493.